



# Shaping of porous mullite green bodies by foaming and thermal gelation of bovine serum albumin

M.L. Sandoval\*, M.A. Camerucci

*Ceramics Division, Research Institute for Materials Science and Technology (INTEMA), CONICET/UNMdP, B7608FDQ, Mar del Plata, Argentina*

Received 28 November 2014; received in revised form 9 January 2015; accepted 10 January 2015

Available online 24 January 2015

## Abstract

The shaping of cellular microstructures of mullite bodies prepared by thermo-gelation of foamed mullite-bovine serum albumin (BSA) suspensions using both a novel forming route and the conventionally reported route were studied. Mullite-BSA and mullite-BSA-methylcellulose (MC) suspensions specific for each route were prepared and then characterized by measuring viscosity. They were subsequently foamed by stirring, and their foaming capacity and foam stability over time were evaluated. Bubble size distributions vs. stand time were obtained by analyzing images captured by confocal laser-scanning microscopy (CLSM). Green bodies were formed by pouring each system into heated molds, by heating and by drying, and were characterized by porosity measurements and microstructural analysis by SEM. The obtained results showed that the use of certain experimental conditions for each route allowed the shaping of homogeneous mullite porous bodies with different microstructural features, namely, ceramic foams with open cells or cellular ceramics with closed cells and thick walls.

© 2015 Elsevier Ltd. All rights reserved.

**Keywords:** Protein-forming; Foaming; Mullite; Pre-firing porous microstructure

## Introduction

In recent years, the increased demand of porous ceramic materials with properties adequate for new applications in highly diverse technological fields has been notable. The development of a porous ceramic material with a specific and controlled microstructure supposes not only the previous microstructural design but also the control of the characteristic parameters for porosity (type of pores, pore morphology, amount of pores and pore size distribution) during the different processing steps since they are determinant aspects of the final properties. However, control of these parameters is not always adequately resolved and for this reason, it constitutes one of the more critical aspects of processing of this type of material.

Among the different types of porous ceramics can be found the classically denominated cellular materials, such as foams, among others. The cellular materials are defined as those formed

by a continuous three-dimensional solid network of struts, which enclose individual cells of a different nature and morphology. These can be either open cells, which have holes in them (cell windows) or closed cells, which do not have windows. These types of materials bring together a unique combination of different properties such as low density, low thermal conductivity, high surface area, and high permeability, all of which determine their specific use in thermal or acoustic insulating, catalyst supports, biomedical implants, scaffolds for cell growth and high efficiency combustion burners, among others.<sup>1,2</sup> In particular, closed-cell materials are needed for thermal applications, while open-cell materials are required for uses such as filters and catalysts. Microstructural features such as density and type of cells, size and morphology of cell, interconnection degree of the network and strut dimension are relevant factors that determine potential applications for these materials,<sup>3</sup> as is the ceramic matrix composition, which must be properly selected.<sup>1–4</sup> Mullite ceramics ( $2\text{SiO}_2 \cdot 3\text{Al}_2\text{O}_3$ ) are important materials due not only to their good mechanical properties at high temperature, but also their low thermal conductivity, low thermal expansion coefficient and good chemical stability.<sup>5–7</sup> The main processing

\* Corresponding author. Tel.: +54 223 4816600; fax: +54 223 4810046.  
E-mail address: [laura.sandoval@fi.mdp.edu.ar](mailto:laura.sandoval@fi.mdp.edu.ar) (M.L. Sandoval).

routes employed to make cellular materials can be divided into three categories, each one including some variations: the replication technique, the direct-foaming technique and the sacrificial template method.<sup>4</sup> Each of these methods presents a series of advantages and disadvantages with respect to the versatility and ease of fabrication, as well as their influence on the microstructure and properties of the developed porous ceramics.

In the direct-foaming method in particular, cellular ceramics are prepared by incorporating a gas (e.g. air) into a ceramic suspension, generally by mechanical stirring. Then, the foamed suspension is consolidated and sintered at high temperature. The forming and sintering processes finally convert the bubbles into pores (cells) among the solid particles of the ceramic matrix. When the film surrounding the bubbles remains intact during the complete consolidation of the suspension, foams with closed bubbles are formed. If the films are partially broken, however, foams with open cells are produced.<sup>3,8</sup> This method is versatile, very simple, inexpensive, and presents some advantages compared to the replica method: a) some shapes, compositions and densities can be easily obtained, b) it allows convenient control over the porous structure of the ceramic material,<sup>9</sup> and c) leads to the development of materials with small cells (smaller than 200  $\mu\text{m}$ ), which can be either open and closed depending on the foaming and processing conditions. Furthermore, unlike the replica method, the struts do not have holes, and they possess a small quantity of defects; in consequence, the mechanical resistance is higher compared to structures obtained by the replica method.<sup>4</sup> However, since the starting system (wet foam) is unstable, the direct-foaming method, in general, requires the addition of a consolidator/binder agent (e.g. some additive that promotes the formation of a gel) in order to allow the consolidation of suspended ceramic particles to occur before the foam destabilization processes begin, which ends up rupturing the bubbles. In most cases, the addition of a surfactant that reduces the surface tension of the gas-liquid interface and stabilizes the gas bubbles inside the ceramic suspension is usually required.<sup>3,4</sup>

In this context, “protein casting”, an innovative non-contaminant colloidal processing of cellular ceramics, is based on thermal consolidation (at temperatures lower than 90 °C) by gelling an aqueous ceramic suspension foamed with globular proteins and the formation of a macro-cellular ceramic structure after removing organics and applying sintering treatments at high temperature. The amount and size of cells in the developed cellular structure depend on the foamed suspension properties and the ability of protein molecules to stabilize the foam before the gelling process occurs (the gas bubbles have to remain occluded in the ceramic suspension for a certain amount of time).<sup>1,3,4,10–13</sup> In this case, a globular protein acts as both a foaming and binder/consolidator agent for the ceramic suspension. These properties are associated with the ability of globular proteins to reduce the surface tension of gas-liquid interfaces and thus stabilize the gas bubbles developed within the suspension (the protein molecules adsorb at the air-water interface and their structure unfolds, which increases the hydrophobicity of the film favoring the foaming), and form a gel in water after heating at 70–80 °C.

Few papers relating to the processing of ceramic materials by protein forming have been published, and most relevant within the last decade. In many of them, albumins as egg-albumin and whey protein concentrate were used; bovine serum albumin, however, was used very little. Many factors related to protein and the other components of the starting suspension, such as protein solubility, protein concentration, ionic strength, pH, type and form of addition of the processing additives and the presence of ceramic particles, influence the foam properties. Due to the highly complex foamed ceramic-protein system, which makes controlling the cellular microstructure difficult, the design and evaluation of various forming routes different from those conventionally reported on are presented as a viable way to obtain cellular materials with controlled microstructures and high homogeneity. These issues and other factors, such as the low heat transfer throughout the porous material and the influence of ceramic particles and organic processing additives on the protein gelation process, which affect the kinetic of ceramic body formation and therefore its final characteristics, reveal the need to investigate in this area. Moreover, it is worth noting that in general, dilute ceramic suspensions (less than 20–25 vol%) were used to prepare cellular materials with very high porosity; however, control over porosity and the problems associated with poor mechanical properties caused by the development of cells with fine walls cannot to be taken lightly.

Based on the above-mentioned concepts, this paper studies the shaping and pre-firing cellular microstructures of mullite bodies developed by direct thermal consolidation of concentrated ceramic suspensions foamed with bovine serum albumin. The inclusion of modifications to the conventionally used processing route is presented as an alternative way to develop materials with controlled and homogeneous pre-firing cellular microstructures.

## Experimental procedure

### *Characterization of the raw materials*

The used ceramic raw material was a high-purity (alkaline impurity level <0.2 wt%) commercial mullite powder (MULS, Baikowski, Annecy, France). The complete characterization of the mullite powder was reported in previous works of the authors.<sup>14,15</sup> Mullite 3/2 (JCPDS File 74-2419) as the primary phase, and  $\alpha$ -alumina (JCPDS File 82-1399),  $\theta$ -alumina (JCPDS File 11-0517), and cristobalite (JCPDS File 77-1317) as secondary phases, were identified by X-ray diffraction (XRD) (X'Pert PRO; PANalytical, the Netherlands; radiation of CuK $\alpha$  at 40 mA and 40 kV). In addition, a low intensity band located in the zone of the more intense diffraction peaks corresponding to the silica polymorphs (20–30°  $2\theta$ ), which are associated with non-crystalline silicate phases, was also observed. The powder density measured by He-pycnometry (Multipycnometer, Quantachrome Co., USA) was 3.07 g/cm<sup>3</sup>. Considering these results, it was inferred that the commercial mullite powder comes from a synthesis process in which the total conversion of the starting mixture (ammonium alum and silica) was not achieved.<sup>16</sup> Moreover, the mullite powder which consists of

small three-dimensional particles, some of them faceted, with equiaxial morphology, presented a high value of specific surface area ( $13.5 \text{ m}^2/\text{g}$ ) (Monosorb; Quantachrome Instruments, USA) and a bimodal particle size distribution (Mastersizer S, Malvern Instruments Ltd., UK) with a low mean volume diameter ( $D_{50} = 1.5 \text{ }\mu\text{m}$ ), a high volume percentage ( $\sim 30\%$ ) of fine particles  $< 1 \text{ }\mu\text{m}$ , and agglomerates up to  $50 \text{ }\mu\text{m}$  in size due to the presence of the very fine particles.

A commercially available high-purity ( $>98\%$ ) bovine serum albumin (BSA; A7906, Sigma-Aldrich, USA) with a density of  $1.27 \text{ g/cm}^3$  measured by He-pycnometry, 583 amino-acids, a molecular weight of  $66.5 \text{ kDa}$ <sup>17</sup> and an isoelectric point (IEP) of approximately  $4.8\text{--}5.2$ <sup>18,19</sup> was used as a foaming and consolidator/binder agent for the ceramic suspension.

Commercially available methylcellulose powder (MC) (M6385-Sigma-Aldrich, USA) with a picnometric density of  $1.28 \text{ g/cm}^3$  measured by He-pycnometry, 1.7 of DS (average number of methoxy groups by glucose unity number) and a molecular weight of  $17 \text{ kDa}$  was used as an additional binder agent.

### Forming of cellular green bodies

#### Design and methodology of consolidation routes

A novel forming route of aqueous mullite suspensions foamed with serum bovine albumin (BSA), designated as the 'Methylcellulose Route' (MCR), was proposed as an alternative route to that previously reported in the literature (called the 'Conventional Route', CR). It was designed with the aim of developing porous green bodies with homogeneous cellular microstructures. With the MCR, a determined amount of methylcellulose was included in the aqueous mullite-BSA suspensions in order to increase the viscosity of the aqueous mullite-BSA suspension, and in consequence, to reduce the performance of foam destabilization mechanisms before the consolidation process (i.e. gelation) occurs. Moreover, a viscosity increase can also cause the reduction of ceramic particles segregation.

For both the CR and MCR, stable aqueous mullite suspensions ( $40 \text{ vol}\%$ ;  $\text{pH}=8.7$ ) were prepared by using the experimental conditions detailed in a previous work of the authors.<sup>14</sup> For the CR, BSA powder was dissolved into the mullite suspension in order to obtain protein concentrations of 5, 10 and 15  $\text{vol}\%$  with respect to the water amount of the suspension. For the other route (MCR), a determined amount of methylcellulose powder was dissolved into the stable mullite suspension in order to obtain concentrations of 0.5 and 2  $\text{wt}\%$ , and then, the resulting suspension was homogenized in a ball mill for 20 min. Finally, the corresponding amount of BSA was dissolved into the mullite-methylcellulose suspension in order to obtain the same protein concentrations (5, 10 and 15  $\text{vol}\%$ ) as in the CR.

The selection of the methylcellulose concentrations was made based on results previously obtained by rheological testing, namely flow curves (apparent viscosity vs. shear rate) and viscoelastic properties as a function of temperature ( $G'$  and  $G''$  vs. temperature) of mullite-BSA (10  $\text{vol}\%$ ) suspensions with different amounts of MC (0,<sup>14</sup> 0.5 and 2  $\text{wt}\%$ <sup>20</sup>). Selection

of the BSA concentration (10  $\text{vol}\%$ ) was based on the fact that the mullite suspension with this amount of protein shows complex-fluid rheological behavior and has intermediate values of apparent viscosity in all the range of shear rates analyzed and thixotropy with respect to remaining BSA concentrations, as was previously reported.<sup>14</sup> In addition, the lowest onset temperature of gelation ( $T_G^0$ ) registered for this system facilitates the evaluation of the viscoelastic behavior of the mullite-BSA-MC suspension as a function of temperature due to the evaporation of water when heating is minimized. Viscosity measurements at room temperature of the aqueous mullite-BSA and mullite-BSA-MC suspensions were performed using a rotational rheometer (MCR 301 Anton-Paar Physics, Germany) under controlled-rate operating modes with a coaxial cylinder sensor (gap, 1 mm). Flow curves were obtained using a three-stage measuring program with a linear increase in shear rate from 0 to  $1000 \text{ s}^{-1}$  in 300 s, 60 s at  $1000 \text{ s}^{-1}$ , followed by a decrease to zero shear rate in 300 s. Dynamic viscoelastic properties were determined by temperature sweep tests (variation of storage,  $G'$ , and loss,  $G''$ , modulus with the increase of temperature) at a heating rate of  $2 \text{ }^\circ\text{C}/\text{min}$ . These oscillatory measurements were carried out using the previously mentioned rheometer operated with a 25 mm-diameter parallel-plate geometry, a gap of 2 mm and a frequency of 1 Hz.

For the analysis of these rheological results, the following issues were considered: (a) a high apparent viscosity value in the range of low shear rates favors the stability of the wet foams (i.e. the foam's ability to retain the gas for a certain amount of time) since the drainage of the liquid phase inside the foam is decreased, and the segregation of ceramic particles is minimized before the consolidation process occurs, and (b) a low apparent viscosity value at high shear rates improves the foam's initial volume or 'foaming capacity' (considered as the capacity of the continuous phase to include air or another gas) and the ability to pour the suspension into molds.

The highest apparent viscosity at  $10 \text{ s}^{-1}$  (low shear rate) was achieved with the mullite-BSA (10  $\text{vol}\%$ ) suspension with 2  $\text{wt}\%$  of MC ( $\eta_{10} = 3920 \text{ mPa s}$ ), which was found to be notably higher than that obtained for the mullite suspension with the same BSA content ( $\eta_{10} = 538 \text{ mPa s}$ ). The viscosity at  $1000 \text{ s}^{-1}$  ( $\eta_{1000}$ ) for the suspension with the lowest concentration of MC (0.5  $\text{wt}\%$ ) was slightly higher ( $\eta_{1000} = 340 \text{ mPa s}$ ) than that corresponding to the suspension without methylcellulose ( $\eta_{1000} = 215 \text{ mPa s}$ ). The global rheological behavior for the mullite-BSA-MC system, which was typically pseudoplastic with low thixotropy, was attributed to the overlapping of the individual rheological behaviors of the mullite-MC system on one hand, and the mullite-BSA system on the other. In spite of these test results, the existence of interactions between BSA and MC mainly with regard to hydrophobic type and hydrogen bonds,<sup>21</sup> which could influence the flow properties of the studied suspensions, was not determined, although their presence cannot be ruled out. Thus, methylcellulose chains interacting with BSA molecules could hinder some structural changes associated with the creation/destruction of structures characteristic of the complex-fluid behavior that was detected for the mullite suspension.

It is well known that aqueous methylcellulose solutions form a reversible elastic gel depending on the solution's concentration. Even though the maximum MC concentration used in this work (0.01 g/ml) was higher than the reported critical concentration ( $c^* \sim 0.003$  g/ml)<sup>22</sup> and MC gel should thus have formed, the complete gelation process did not occur (the gel formation was not visually observed when the oscillatory rheological test finished). This indicates that, for the MC concentrations used, the polysaccharide does not act as an additional gelling additive, but behaves mainly as an additional binder of ceramic particles. However, the formation of methylcellulose and BSA aggregates due to intermolecular associations, mainly hydrophobic (protein with negative net charge and neutral polysaccharide), was assumed due to the fact that  $G'$  slightly increased by increasing the temperature. This consideration was supported by the fact that in all the range of analyzed temperatures,  $G''$  was always lower than  $G'$  and  $G'$  was slightly higher than reported values for highly diluted systems ( $c < c^*$ ).<sup>22</sup>

For both studied routes, the corresponding aqueous suspensions, i.e. mullite-BSA or mullite-BSA-MC, were foamed by mechanical stirring using the experimental conditions determined in a previous work.<sup>14</sup> Mullite-BSA or mullite-BSA-MC disks (labeled as CR and MCR disks) were formed by pouring the corresponding foamed suspension into stainless steel cylindrical molds (diameter = 2.20 cm; height = 1.00 cm) previously heated at 60 °C and covered on the inside with PTFE (polytetrafluoroethylene, Teflon) adhesive tape to facilitate the removal of the samples and prevent the generation of defects due to deficient wetness. They were then heated in an electric stove (UFP 400, Memmert, Germany) at 80 °C for 3 h. Once the consolidation was finished, the samples were taken out of their molds and dried at 50 °C for 12 h. The temperature used in the thermal consolidation process was previously selected from dynamic rheology measurements as a function of temperature.<sup>20</sup> This temperature (80 °C) was slightly higher than the onset temperatures of gelation determined for mullite-BSA (10 or 15 vol%) and a little lower than that for mullite with 5 vol% of protein to avoid water evaporation during the consolidation of the foamed system. Moreover, this temperature enables the gelation kinetic of the albumin to increase, thus decreasing the necessary time to achieve a uniform consolidation temperature throughout the total volume of the suspension; in consequence, this minimizes any possible thermal gradients in the samples, which can produce microstructural inhomogeneity, particularly with regard to cell size distribution as well as defects associated with the differential volumetric shrinkage.

Finally, the effect of slightly lower ceramic loading in the starting suspension used for MCR on the developed green microstructures was also evaluated. A lower amount of mullite in the suspension favors the development of microstructures with higher porosity. For this purpose, an aqueous mullite suspension with 35 vol% of total ceramic loading, 10 vol% of BSA and 0.5 wt% of MC was prepared using the same experimental conditions and methodology as with the more concentrated suspension (40 vol%). As for the shaping of disks, the experimental procedure used in this case was already specified for forming disks by MC using a suspension with 40 vol% of solids.

### Evaluation of physical properties of the foamed suspensions

In the context of the consolidation method studied, the evaluation of the wet foam properties is a key point since they determine the features of the cellular microstructure. Protein solubility, protein concentration, ionic strength, pH, type and the methodology for adding the processing additives, and the presence of ceramic particles are some of the many factors that have an influence on foam properties. In particular, the presence of a polysaccharide in a ceramic-protein suspension can significantly affect the properties of the generated foam since it also has the ability to accumulate in the air-water interfaces, thus reducing their surface tension. Thus, the effect on the foaming properties by adding methylcellulose (0.5 and 2 wt%) to the aqueous mullite-BSA (10 vol%) suspensions was analyzed.

Foaming properties were characterized by the foaming capacity and foam stability over time. The foaming capacity or initial foam volume was evaluated using the volumetric method.<sup>14</sup> The value of the parameter called *Overrun%* (relative error  $\sim 10\%$ ) at zero time was taken as the foaming capacity of the system. In this article, the following equation was considered:

$$\text{Overrun}\% = 100 \left( \frac{V_T - V_i}{V_i} \right) \quad (1)$$

where  $V_T$  is the total volume (foam volume plus liquid volume) and  $V_i$  is the initial liquid volume.<sup>18,23–26</sup> Considering that, in the case of ceramic systems, the measurements of the corresponding volumes cannot be made accurately since the ceramic particles suspended in the liquid phase hide the bubbles, the variation of *Overrun%* as a function of time was not considered when evaluating the stability of wet ceramic foams. In contrast, the study of the stability of foamed ceramic-protein systems was carried out using the conductimetric technique, which is based on the monitoring of change in the foam's electric conductivity ( $C_t$ ) as a function of stand time ( $t_s$ ). In this case, the water surrounding the bubbles acts as the main conductor medium.<sup>27–30</sup> Thus, the electric conductivity of the foam measured immediately after producing each foamed system ( $C_i$ ) and foam electric conductivity as a function of stand time,  $t_s$  ( $C_t$ ) were used to characterize the foam density stability (FDS%) (2) and the time to half collapse,  $t_{1/2}$  (time in which the foam density stability decreased by 50%).<sup>31</sup>

$$\text{FDS}\% = 100 \frac{C_t}{C_i} \quad (2)$$

Also, the variation of another parameter with the stand time, namely the foam wetness ( $\Phi_{FW}$ ), which is defined as the ratio between the amount of liquid inside the foam and the foam volume plus the liquid volume inside the foam, can be determined by electric conductivity method using the following Eq. (3):<sup>27–30,32</sup>

$$\frac{C_t}{C_s} = \frac{2\Phi_{FW}}{3 - \Phi_{FW}} \quad (3)$$

where  $C_s$  is the electric conductivity of the liquid medium (i.e. aqueous protein solution).

Tests were performed using a conductivity meter (GW Instek SFG-1013; Digital Multimeter Rigol DM3062) and an electrode



of stainless steel parallel Plates  $12.5 \times 12.5 \text{ mm}^2$  and 0.3 mm thick with a separation distance of 25.5 mm. An AC carrier effective voltage of 1.0 V was applied across the electrode at a frequency of 25 kHz. The used experimental conditions and procedure were the same as reported in a previous work of the authors.<sup>14,29</sup>

Number-weighted bubble size distributions of foamed mullite-BSA and mullite-BSA-MC suspensions as a function of stand times (0, 10 and 30 min) were obtained by analyzing images (Image-Pro Plus 7.0, Media Cybernetics) captured by CLSM (Nikon C1, Japan). The used experimental conditions were reported in a previous work.<sup>14</sup> The characteristic parameters, such as mean bubble diameters,  $D_{50}$  (bubble diameters for 50% of bubbles) and distribution width (this parameter was taken as  $W = (D_{90} - D_{10})/D_{50}$  where  $D_{90}$  and  $D_{10}$  are the bubble diameters for 90 and 10% of bubbles, respectively) were determined by analyzing  $\sim 600$  objects.

### Characterization of green bodies

Densities ( $\rho_g$ ) of green bodies were determined by immersion in Hg (Archimedes method), and porosities ( $\%P_g$ ) were calculated from  $100 \cdot (1 - \rho_g/\rho_m)$  where  $\rho_m$  is the pycnometric density of the mullite-BSA or mullite-BSA-MC powdered mixtures. In addition, relative densities ( $\rho_{r-g}$ ) as  $\rho_g/\rho_m$  ratio were obtained. The pycnometric density value corresponding to each powder mixture ( $\rho_m$ ) was calculated by the mixing rule using the pycnometric density of each of the mixture components (mullite, BSA, and MC) and their volume fractions. The obtained values for mullite-BSA mixtures were 3.05, 3.03 and 3.00 g/cm<sup>3</sup> for 5, 10 and 15 vol% of BSA, respectively, while for mullite-BSA-MC mixtures with 0.5 wt% of MC, these values were 3.03 g/cm<sup>3</sup> (BSA 5 vol%), 3.02 g/cm<sup>3</sup> (BSA 10 vol%) and 3.00 g/cm<sup>3</sup> (BSA 15 vol%), and when the addition of MC was of 2 wt%, 3.05 g/cm<sup>3</sup> (BSA 5 vol%), 3.02 g/cm<sup>3</sup> (BSA 10 vol%) and 3.00 g/cm<sup>3</sup> (BSA 15 vol%) were the obtained values.

The microstructural analysis of the green materials was performed by SEM (JSM-6460, JEOL) on fracture surfaces of the disks. Cell size distributions were obtained from the analysis of the SEM images by using image analysis software (Image-Pro Plus 7.0, Media Cybernetics). The characteristic parameters, mean cell diameter ( $D_{50}$ ) and distribution width (this parameter was considered as  $W = D_{90} - D_{10}/D_{50}$ , where  $D_{90}$  and  $D_{10}$  are the cell diameters for 90 and 10% of cells, respectively) were determined. Moreover, average window size and the percentage of each type of cell (open and closed) were also determined.

## Results and discussion

### Evaluation of physical properties foamed suspensions

Because of the existence of different types of interactions between proteins and polysaccharides, which may be the cause of synergistic effects on the formation and stabilization of wet foams, a summary of the behavior of foamed aqueous protein-polysaccharide systems is given before presenting the obtained results. When a protein adsorbs at the air-water interface in

the presence of polysaccharide molecules under conditions of limited thermodynamic compatibility, such as in the case under study, three phenomena can occur: (a) the polysaccharide (MC) adsorbs at the interface, in competition with the protein (competitive adsorption), (b) the polysaccharide interacts with the adsorbed protein, mainly by hydrogen bonding and hydrophobic associations, forming complexes, or (c) the polysaccharide concentrates the adsorbed protein due to the existence of a limited thermodynamic compatibility. The first two mechanisms suppose that the anchorage of the polysaccharide at the interfacial film takes place first, and then, the exclusion effects between both biopolymers (i.e. BSA and MC) are produced. Thus, a more concentrated film would be developed, which would lead to a decrease in the surface tension. However, even when the polysaccharide is not adsorbed at the interface, the existence of low thermodynamic compatibility between the protein and polysaccharide could lead to an increase in the concentration of the adsorbed protein by a depletion mechanism. Therefore, the osmotic driving force that favors the protein aggregation could also involve the decrease in the surface tension.<sup>33</sup> Since the methylcellulose has a strong tendency to accumulate at the air-water interface, the existence of a mechanism leading to anchorage of the polysaccharide is considered highly probable.

The obtained values of *Overrun%* at  $t_s = 0$  indicate that the foaming capacity (211%) of the aqueous mullite-BSA (10 vol%) suspension notably decreased with the increase in the MC amount. Thus, the addition of 0.5 wt% of methylcellulose caused the foaming capacity to decrease 33%, obtaining an *Overrun%* value of 140%, while for 2 wt%, the *Overrun%* was equal to 100%, which represents a reduction of 48%, in comparison with the value obtained for mullite-BSA foam with the same protein content. These results reveal that the foaming capacity of suspensions with MC would depend mainly on their viscosity, although the influence to a variable degree of other additional factors (e.g. the foam formation kinetic) on this parameter cannot be ruled out. The apparent viscosities at  $1000 \text{ s}^{-1}$  ( $\eta_{1000}$ ) for the aqueous mullite-BSA (10 vol%) suspension with 0.5 and 2 wt% of MC were higher ( $\eta_{1000}$  0.5% MC = 340 mPa s and  $\eta_{1000}$  2% MC = 567 mPa s) than those corresponding to the suspension without a polysaccharide ( $\eta_{1000} = 215 \text{ mPa s}$ ), even more so with higher MC concentrations, which leads to a decrease in the foaming capacity of systems with methylcellulose. It was also reported that certain interactions between the protein and the polysaccharide can decrease the fall rate of the interfacial tension, and a lower volume of foam would be formed in consequence.<sup>33</sup>

Regarding the variation of foam wetness ( $\Phi_{FW}$ ) as a function of stand time (Fig. 1a.), the addition of methylcellulose into the mullite-BSA suspension led to an increase in the  $\Phi_{FW}$  values throughout the entire range of analyzed stand times, indicating that for both MC concentrations, wetter foams ( $\Phi_{FW} > 0.45$ ) were generated, which can be attributed mainly to the interactions between polysaccharide and water molecules. For both MC concentrations, and even more so for 2 wt% of MC, the decrease in  $\Phi_{FW}$  caused by the increase in stand time was less pronounced when compared to the suspension without MC, with obtained values higher than 0.3 at 30 min. These results indicate that in

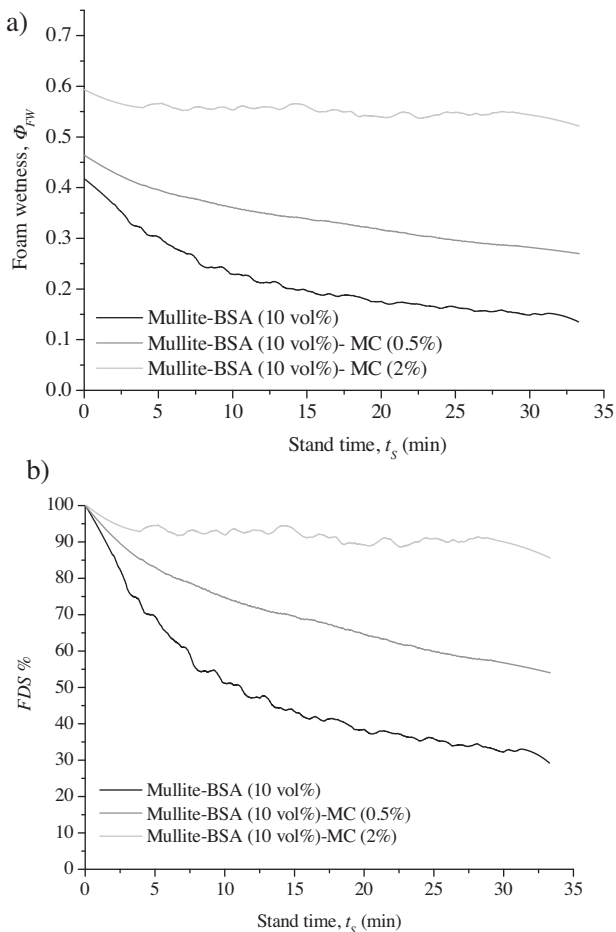


Fig. 1.  $\Phi_{FW}$  (a) and FDS% (b) as a function of the stand time,  $t_s$  for foamed mullite-BSA (10 vol%) suspensions with different MC concentrations (0, 0.5 and 2 wt%).

these foams, the drainage rate of the liquid phase as well as the drainage itself was lower than that recorded for the suspension without MC.

The effect of the cellulosic additive on the drainage rate of foams can be clearly appreciated from the analysis of the FDS% as a function of the stand time (Fig. 1b). The decrease in this parameter over time due to the increase the MC content was much lower. Moreover, for both MC concentrations, to a greater extent for 2 wt%,  $t_{1/2}$  values were significantly higher (>30 min for the suspension with 0.5 wt% of MC and  $\gg$  35 min for the suspension with 2 wt%) than the value obtained for the suspension without MC (11 min), which exceed the analyzed time range, which is why they could not be accurately determined.

Based on the theoretical considerations mentioned, the existence of mechanisms which lead to anchoring the methylcellulose at the interface or directly to the protein would partly explain the increased stability of the foams obtained from mullite-BSA-MC suspensions with respect to those formed without MC. Moreover, the formation of very elastic methylcellulose interfaces, along with a high liquid medium viscosity, would contribute to improving the foam's stability. Thus, the increase in foam stability generated by the presence of methylcellulose can be mainly attributed to the direct incidence of this

last additive together with the effect produced by the significant increase in the suspension's apparent viscosity at low shear rates (e.g.  $\dot{\gamma} = 10 \text{ s}^{-1}$ ) ( $\eta_{10}$  MC 0 wt% = 538 mPa s,  $\eta_{10}$  MC 0.5 wt% = 1900 mPa s and  $\eta_{10}$  MC 2 wt% = 3920 mPa s). The influence of both factors was much greater for the suspension with the highest amount of MC, which was the system that achieved maximum stability.

In addition, bubbles size distributions were obtained by analyzing images from confocal microscopy corresponding to foams generated from mullite-BSA (10 vol%)-MC (0, 0.5 and 2 wt%) suspensions for different stand times ( $t_s = 0, 10$  and 30 min). Typical confocal microscopy images of the foams obtained from mullite-BSA-MC suspensions are shown in Fig. 2.

The mean bubble diameter ( $D_{50}$ ) and width ( $W$ ) values of each distribution (Fig. 2), were lower than those obtained for mullite foams with an equal concentration of BSA and without methylcellulose at all the evaluated stand times. Moreover, for the two MC concentrations, the increase in stand time caused both parameters ( $D_{50}$  and  $W$ ) to vary less than those for the foams without MC. The  $D_{50}$  values corresponding to the two MC concentrations were very similar to each other, whereas  $W$  was lower at each stand time for the suspension with 2 wt% of MC.

These results are consistent with the higher stability of the foams prepared from suspensions with methylcellulose, although they also suggest that the overall destabilization mechanism does not change significantly, as determined in previous work<sup>14</sup> on foams formed without MC: during the first few minutes, the drainage of the liquid phase prevails, although to a lesser extent than with foams without methylcellulose. By increasing time, the Ostwald ripening, which is a coarsening process caused by interbubble gas transport (disproportionation) and the coalescence of neighboring bubbles due to the rupture of interbubble lamellae (film rupture) and the joining of two bubbles to generate a larger bubble, plays a more preponderant role.

#### Characterization of green bodies

After the drying treatment, green disks formed by CR using the mullite suspensions with 10 and 15 vol% of BSA displayed a visually homogeneous structure throughout its entire thickness and experimented shrinkage of 1.5% in diameter and 6% in height. However, very defective disks, which in most cases presented voids inside and very low cohesion among particles, were obtained when the suspension with the lowest amount of BSA (5 vol%) was used. A typical SEM micrograph corresponding to the complete fracture surface of disks prepared by RC using the lowest BSA concentration (5 vol%) is shown in Fig. 3.

In this case, very different microstructures in the upper and bottom regions of the disk fracture surface were observed, which indicates that these materials resulted in being highly inhomogeneous. In the upper region, close to the free surface, three layers were observed, each constituted by cells differentiated from one another by their size. Thus, in the layer adjacent to the free surface of the disk, a mean cell size of  $69 \pm 2 \mu\text{m}$  was

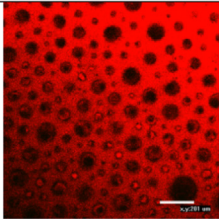
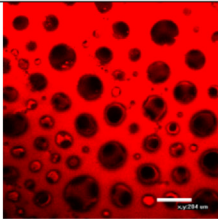
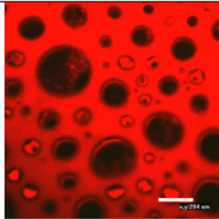
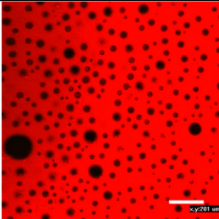
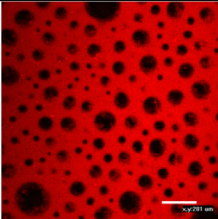
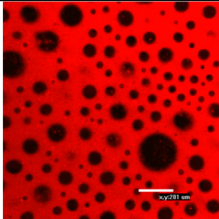
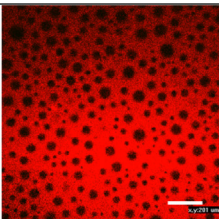
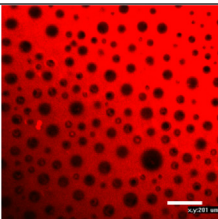
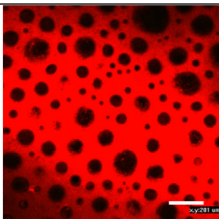
[MC] (wt%)	0 min	10 min	30 min
0%			
$D_{50}$ (mm)	0.06±0.01	0.09±0.01	0.11±0.02
W	1.3±0.1	1.5±0.1	1.5±0.1
0.5%			
$D_{50}$ (mm)	0.03±0.01	0.05±0.01	0.06±0.01
W	1.0±0.1	1.2 ±0.3	1.3±0.1
2%			
$D_{50}$ (mm)	0.04±0.01	0.05±0.01	0.06±0.01
W	1.0±0.1	1.0±0.1	1.2±0.3

Fig. 2. Typical confocal microscopy images of foamed mullite-BSA (10 vol%)-MC (0, 0.5 and 2 wt%) suspensions for different stand times (0, 10 and 30 min). Bar = 200 μm.

determined; the following layer displayed cavities with a mean size ( $260 \pm 90 \mu\text{m}$ ) notably higher than the former, and in the last porous layer, cells with sizes similar to those determined for the first layer had developed. Unlike what was observed in the

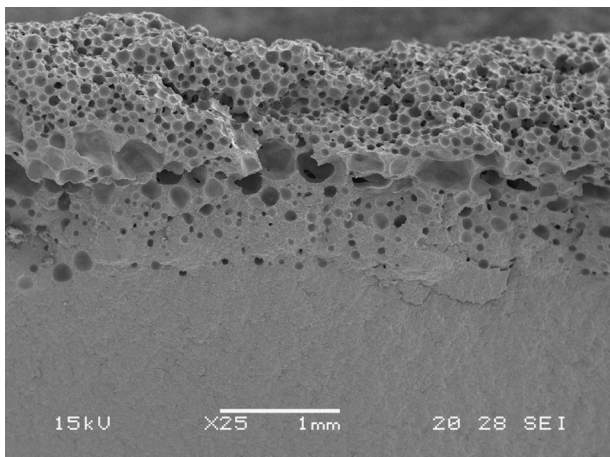


Fig. 3. Typical SEM micrograph of fracture surface of disks prepared by CR using the mullite-BSA (5 vol%) suspension.

upper region of the disk fracture surface, the presence of cells was not observed in the microstructure of the bottom region. The occurrence of a considerable foam destabilization due to the fact that the aqueous mullite suspension with 5 vol% of BSA displayed the lowest viscosity and generated the less stable foam in relation to the systems with higher concentrations of BSA (10 and 15 vol%) could explain the development of this type of microstructure. Thus, foam destabilization facilitated the ascent of a great amount of large bubbles associated with the change of the hydrostatic pressure, as well as the collapse of much of them at the surface in contact with the atmosphere. In this way, small bubbles remained in the outer layer, while in the following layer, other larger bubbles were trapped due to the premature consolidation of the layer brought on by its location in the upper region of the disk, at higher temperature. Moreover, the large amount of surface bubbles produced a significant decrease in thermal conductivity through the formed layer, which prevented the development of the gel inside the body and resulted in a poorly consolidated inhomogeneous material; these disks were thus not characterized by density measurements. Based on these results, the system with 5 vol% of BSA was discarded for posterior study.



Table 1  
Green density ( $\rho_g$ ), total porosity ( $P_g$ ) and relative density ( $\rho_{r-g}$ ) values of green disks prepared by CR and MCR.

[MC] (wt%)	[BSA] (vol%)	$\rho_g$ (g/cm <sup>3</sup> )	$P_g$ (%)	$\rho_{r-g}$
0	10	0.85 ± 0.05	72 ± 2	0.28 ± 0.02
	15	0.78 ± 0.07	74 ± 2	0.26 ± 0.02
	5	0.92 ± 0.03	70 ± 1	0.30 ± 0.01
0.5	10	1.11 ± 0.04	63 ± 1	0.36 ± 0.02
	15	1.18 ± 0.04	61 ± 1	0.39 ± 0.01
	5	1.15 ± 0.06	62 ± 2	0.38 ± 0.02
2	10	1.09 ± 0.04	64 ± 1	0.36 ± 0.01
	15	1.16 ± 0.04	61 ± 1	0.39 ± 0.01

In contrast, disks obtained by MCR displayed good surface quality without any deformation or cracks. The dimensions resulted in being similar to disks formed by CR. In this case, disks underwent shrinkage in diameter slightly less (0.5%) than for disks obtained by CR and were rather similar in height (6.6%) to disks also shaped by CR.

In Table 1, green density ( $\rho_g$ ), total porosity ( $P_g$ ) and relative density ( $\rho_{r-g}$ ) values obtained by CR and MCR are shown.

According to the values of these parameters, disks obtained by CR displayed high porosity. The use of the highest protein amount did not determine a significant difference among the obtained total porosity values. The relative density values were lower than the superior limit of values usually reported in the literature (<0.5) for cellular materials like foams.<sup>3</sup> On the other hand, the total porosity developed in the disks obtained by MCR was somewhat lower than that of the disks prepared by the other route. This result agrees in part with the fact that in the presence of methylcellulose, a lower foam volume was obtained. Based on porosity values, the methylcellulose concentration was not a determining factor in the porosity since in every disk except for those prepared from mullite-BSA (5 vol%)-MC (0.5 wt%), which displayed porosity in the range of values registered for disks prepared by CR, the obtained porosities (61–64%) were quite similar. The results show that the addition of methylcellulose into the mullite-protein suspension facilitated the development of a porous microstructure whose total volume of pores changed slightly by varying the polysaccharide and protein concentrations. In these materials, relative densities lower than 0.39 were determined.

Typical SEM micrographs of the fracture surface of materials prepared by CR and MCR are shown in Fig. 4.

When the protein concentrations were 10 and 15 vol%, disks prepared by CR displayed a cellular microstructure with features typical of a ceramic foam composed of a continuous three-dimensional solid network of struts with an acceptable packing degree and cells with an almost spherical morphology separated by thin solid walls, as is shown in Fig. 4. These microstructural features were in agreement with the low relative densities obtained (Table 1). Microstructures with a higher homogeneity degree, as to the distribution of cells and their characteristics throughout the thickness of the disk, than that obtained in the material prepared with the 5 vol% of protein were developed. Moreover, the microstructural homogeneity became greater by increasing the BSA concentration. In neither case did a

significant segregation of ceramic particles and/or bubbles occur. These results can be attributed to the improved stabilization of the foamed suspension and properties of the viscoelastic protein film which covers the bubbles when the BSA content is increased.

In all the materials prepared by MCR, the development of a cellular microstructure containing cells with a spherical morphology and having thicker walls than cells formed in disks prepared by CR was observed. In general, in these materials, struts with a good packing degree and a low percentage of defects appear in a more isolated form; that is, the formation of a continuous three-dimensional solid network of struts is not clearly distinguished (Fig. 5).

On the other hand, and independent of BSA and MC concentrations, a good mullite particle packing was observed in solid walls surrounding cells as much as in the matrix of every disk.

The microstructures developed displayed good homogeneity and ended up being quite similar, although cell size was strongly dependent on the BSA concentration. Cell sizes decreased when increasing the BSA amount although, for materials prepared with 5 and 10 vol% of BSA, obtained cell sizes were very similar. On the other hand, an increase in the MC concentration also led to a decrease in the cell sizes. This effect was less pronounced when the protein content was increased to 15 vol%.

Cumulative distribution curves of cell diameter corresponding to the materials prepared by both studied routes are shown in Fig. 6.

The  $D_{50}$  values for materials consolidated by CR using 10 and 15 vol% of BSA were  $95 \pm 2 \mu\text{m}$  and  $70 \pm 4 \mu\text{m}$ , respectively, while  $W$  values (distribution width) were not very different ( $1.2 \pm 0.1 \mu\text{m}$  and  $1.5 \pm 0.5 \mu\text{m}$ , respectively), even though for 15 vol% of BSA  $W$  achieved the highest value. These results and the spherical morphology of cells were consistent with determined parameters ( $D_{50}$  and  $W$ ) for bubble size distributions corresponding to foamed mullite-BSA (10 and 15 vol%) suspensions for stand times of 10 and 0 min, respectively.<sup>14</sup> This fact would confirm that the stability of the foam prepared with 15 vol% of protein did not significantly vary during the thermal treatment of consolidation.

Concerning the materials prepared by MCR, the mean cell diameters ( $D_{50} = 42 \pm 1$ ,  $40 \pm 2$  and  $26 \pm 2$  for mullite disks with 0.5 wt% of MC and 5, 10 and 15 vol% of BSA, respectively;  $27 \pm 1$ ,  $29 \pm 1$  and  $21 \pm 1$  for mullite disks with 2 wt% of MC and 5, 10 and 15 vol% of BSA, respectively) turned out to be quite lower than those of the materials prepared by CR. In addition, in the case of the systems with 10 vol% of protein and 0.5 and 2 wt% of methylcellulose, the values of this parameter were in agreement with the mean bubble diameters (Fig. 2) corresponding to the foamed systems for stand times of 0 min. Regarding the  $W$  parameter, the values obtained for these systems were somewhat higher ( $1.6 \pm 0.1$ ,  $1.5 \pm 0.1$  and  $1.6 \pm 0.1$  for mullite disks with 0.5 wt% of MC and 5, 10 and 15 vol% of BSA, respectively;  $1.8 \pm 0.2$ ,  $1.7 \pm 0.1$  and  $1.6 \pm 0.1$  for mullite disks with 2 wt% of MC and 5, 10 and 15 vol% of BSA, respectively) than those corresponding to the systems used for CR and the foamed systems with MC in the range of analyzed stand times.



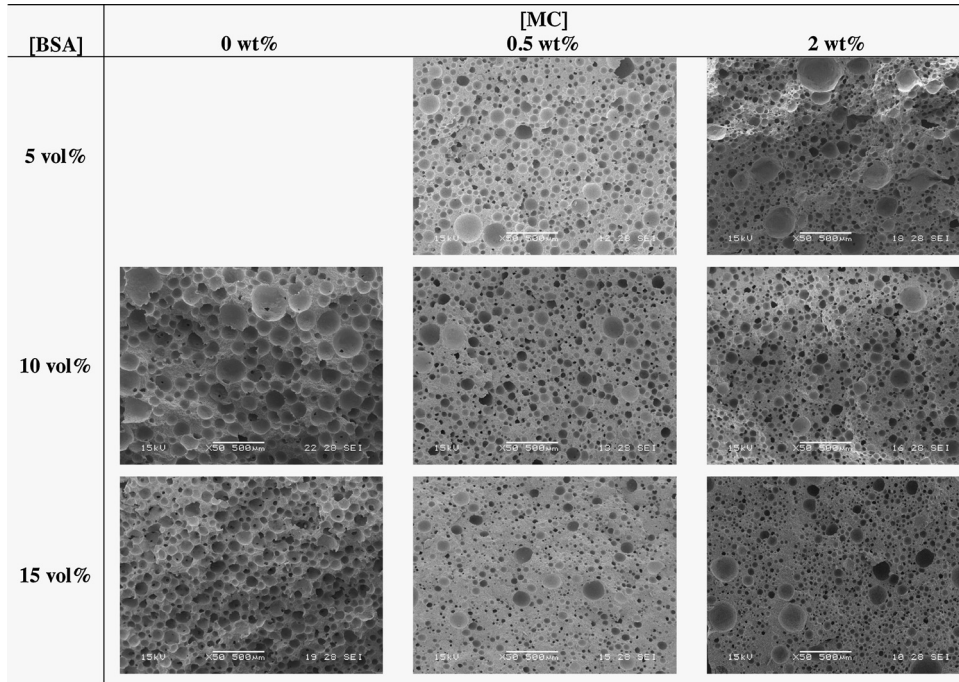


Fig. 4. SEM micrographs of fracture surfaces of disks prepared by CR (10 and 15 vol% of BSA) and MCR (5, 10 and 15 vol% of BSA, and 0.5 and 2 wt% of MC).

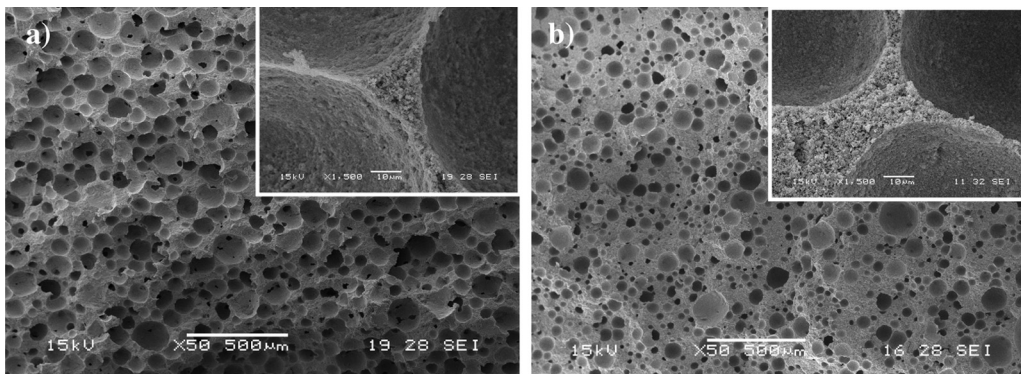


Fig. 5. SEM micrographs showing in detail a strut for materials formed by (a) CR and (b) MCR.

On one hand, the correlation between the  $D_{50}$  values would indicate that the stabilization of foamed mullite-BSA-MC suspensions was not affected during the thermal consolidation process. On the other hand, the  $D_{90}$  values (78 and 63  $\mu\text{m}$ , for materials prepared with 10 vol% of BSA and 0.5 or 2 wt% of MC, respectively) and  $D_{10}$  values (19 and 13  $\mu\text{m}$ , for materials

prepared with 10 vol% of BSA and 0.5 or 2 wt% of MC, respectively) for the cell size distributions of the systems with MC were of the order or slightly lower, respectively, than those determined for the corresponding foamed systems ( $D_{90} = 0.06 \pm 0.01$  mm and  $D_{10} = 0.03 \pm 0.01$  mm, for both MC amounts). Taking into account these aspects,  $W$  values measured for the cell population

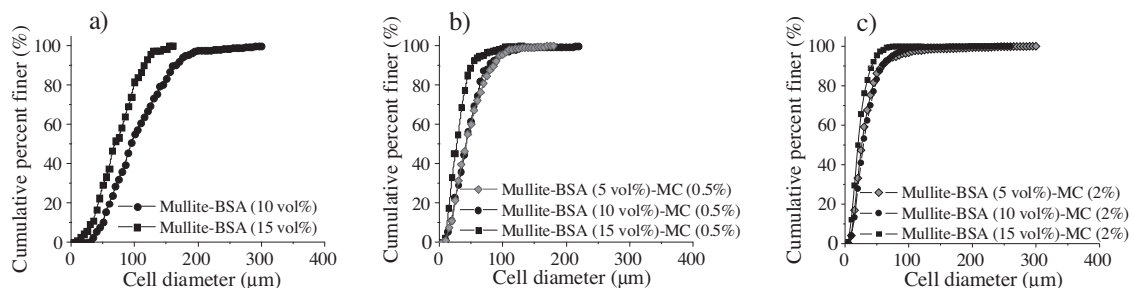


Fig. 6. Cumulative cell diameter distributions for materials formed by CR (a) and MCR using 0.5 wt% (b) and 2 wt% (c) of methylcellulose.

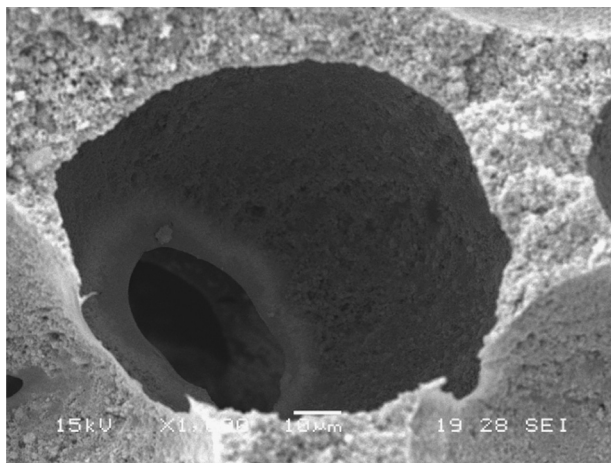


Fig. 7. SEM micrograph showing a cell which contains a window (open cell) for a material prepared by CR using 15 vol% of BSA.

belonging to green disks could be explained considering that for the analysis of confocal images, the totality of bubbles with sizes lower than  $20\ \mu\text{m}$  could not have been quantified since these images were captured using low magnification ( $20\times$ ) to generate a large field of view and quantify a population comprising a great number of bubbles.

Another important microstructural characteristic of the developed porous materials is the presence of windows in some of the cavities interconnecting neighboring cells, which originate from the rupture of the material constituting the wall that separates them. In Fig. 7, a typical open cell containing a window is shown.

The higher percentages of windows, the higher cell interconnection degree, and consequently, the final open porosity will be higher. For microstructures developed using foamed suspensions with 10 and 15 vol% of BSA, a similarly high percentage of windows (i.e. ratio between the number of cells with windows and the number of total cells) was observed for both materials (27 and 30% for materials prepared with 10 and 15 vol% of BSA, respectively). Taking into account that the mullite suspension with 10 vol% of protein displayed lower viscosity and stability than the suspension with 15 vol% of BSA, the percentage of windows present in the formed material using the former suspension should have been higher than that obtained for the green bodies with the greatest amount of BSA. This discrepancy could be justified considering that for the analysis of this parameter in the material with 10 vol% of BSA, an important number of fragmented cells, which might have contained windows, were not taken into account in the percentage calculation. On the other hand, the average window size was independent of the BSA content used ( $18 \pm 1\ \mu\text{m}$  and  $19 \pm 3\ \mu\text{m}$ , for 10 and 15 vol% of BSA, respectively), and the size of the cells in which the windows were found.

Several factors are responsible for the generation of windows; among them, the use of low solid loading and/or a suspension with low viscosity as well as the occurrence of a fast coarsening process on the part of bubbles before reaching good particle packing on the bubble surface and producing system gelation, which enables a highly interconnected structure of pores to be developed. For these systems, it was assumed that the moderate

viscosity and in consequence, the moderate stability of starting foamed suspensions was the main factor that determined the amount of windows developed in these materials. The possible rupture of the wall of some cells during the drying process could also be an additional factor that would contribute to increasing the connectivity of cells in these materials, in particular, for those prepared with the lowest BSA content (softer gel). The obtained results indicate that, even though these cellular materials were developed from foams with thin films, which achieved a moderate degree of stability that depended on the protein content, the employed methodology and experimental forming conditions are considered acceptable in the context of processing of these types of materials.

Regarding the materials prepared by MCR, the window percentage was notably lower than that determined for disks formed by CR, which would indicate that the cavities possess a low degree of interconnection. The determined values depended on the content of both organic agents (MC and BSA) in the starting suspensions. For materials prepared with 5 vol% of BSA and the lowest MC percentage (0.5 wt%), the highest window percentage (14%) was determined (the remaining materials presented only 5%). Concerning the average window size, such as in the case of disks prepared by CR and independent of cell size, no significant differences were observed among the average values corresponding to materials prepared with the different amounts of BSA and MC; the obtained values were between 5 and  $6\ \mu\text{m}$ .

The developed microstructural characteristics are consistent with the rheological behavior of mullite-BSA-MC suspensions and the physicochemical and viscoelastic properties of these foamed suspensions. The formation of cells that are mainly closed is consistent with the fact that the wider and stronger the wall is, the lower the probability that interconnections will form among cavities. The obtained results also confirm that the action of the methylcellulose operating not only directly at the air–water interface but also indirectly inside the starting suspension improves the foamed system's stability, which might collaborate in the development of microstructures with mainly closed cells.

Finally, disks obtained by this route (MCR) using aqueous mullite suspensions with 35 vol% of total ceramic loading were characterized. This suspension displayed apparent viscosities of 272 and  $65\ \text{mPa}\cdot\text{s}$  at 10 and  $1000\ \text{s}^{-1}$  respectively, which were notably lower than the viscosities of every ceramic-protein suspension prepared with 40 vol% of solids and higher than that of the aqueous mullite suspension (40 vol%), and even more so for the considered lowest shear rate ( $10\ \text{s}^{-1}$ ). Based on these results, it is expected, on the one hand, that from this system, a larger foam volume is formed (greater foaming capacity), and on the other hand, that this foam has lower stability in comparison with systems prepared with a higher solid loading. In this case, after the drying treatment, disks displayed a structure that was visually very similar to that observed in dried disks prepared by CR using 10 and 15 vol% of BSA. Moreover, no defects, cracks or geometrical deformation was observed. In addition, they presented good cohesion among the particles and the surface finish.

As was expected according to the data reported in the literature,<sup>34</sup> green and relative densities turned out to be lower



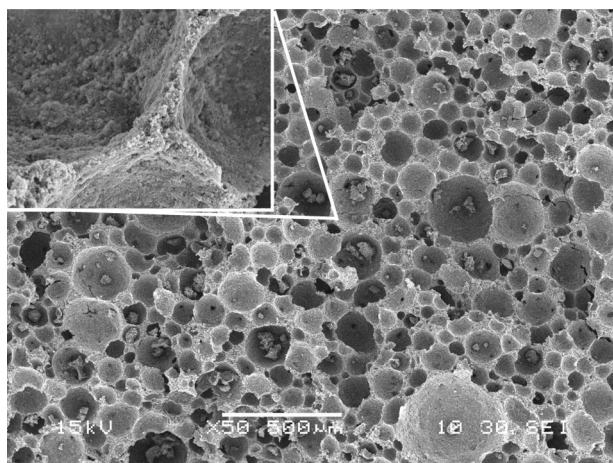


Fig. 8. SEM image of the typical microstructure of fracture surface of disks obtained by MCR (35 vol% of ceramic loading), and detail of a strut.

than those corresponding to the disks formed by CR (Table 1):  $\rho_g = 0.60 \pm 0.03 \text{ g/cm}^3$  and  $\rho_{r-g} = 0.20 \pm 0.01$ . In addition, the total porosity was  $80 \pm 1\%$ , which is higher than that obtained in green materials prepared from more concentrated systems.

In Fig. 8, a typical SEM micrograph of the fracture surface of disks prepared with 35 vol% of ceramic loading is shown.

As can be observed in the image in Fig. 8, the material displays a very different microstructure than that developed in materials prepared by MCR using the same BSA and MC concentrations but with a higher solid content. The material prepared with the lowest solid loading presented a cellular microstructure with characteristics of ceramic foam similar to that developed in materials obtained by CR using 40 vol% (Fig. 5). The formation of a continuous solid three-dimensional network of struts and nearly spherical cells separated by solid thin walls resembling those present in disks prepared by CR, which in some cases also appeared fragmented, was observed. Furthermore, the packing degree of the ceramic matrix was somewhat lower than that in disks formed by CR, which is consistent with the use of a suspension with lower solid loading.

Cells displayed a mean size of  $64 \pm 3 \mu\text{m}$ , which was higher than that obtained in disks prepared by MCR with the same BSA and MC content but employing the more concentrated suspension, and lower than that corresponding to material formed by CR from the system with the same concentration of protein. Regarding the percentage of windows in these materials, the value (28%) was similar to that determined for materials prepared by CR (30%) and rather higher than the values obtained by MCR with higher solid loading and the same contents of BSA and MC (5%). An average window size of  $9 \pm 6 \mu\text{m}$  was determined in this material. As in the other materials, this size was independent of the cell size. The wide dispersion of this value could be mainly associated with the development of a certain number of cells with very thin walls constituted by poorly packed particles. This fact suggests that from the suspension with 35 vol% of solids, and even in presence of methylcellulose, foams with stability somewhat lower than that of the foam prepared with the more concentrated suspension and the same amount of MC were developed. Moreover, based on the

microstructural characteristics of these green materials and the fact that a lower number of mullite particles with respect to the more concentrated suspension were available (suspension with lower solid loading), it can be inferred that in this system, the anchoring of the methylcellulose to the protein would contribute to a lesser extent to foam stability.

## Conclusions

Cellular mullite green bodies with good surface quality, without cracks or deformations and with homogenous microstructures, were shaped using both the proposed route and the route conventionally reported, both of which are based on the thermogelation of foamed mullite suspensions with bovine serum albumin.

The use of methylcellulose as an additional binder of the ceramic suspension, even though it generated a lower foam volume, made possible the development of foams that were wetter and stable than those generated from the systems with only protein. These facts were attributed mainly to the increase in the viscosity suspension, although the possible anchoring of the polysaccharide at the air-water interface or directly to the protein molecules, together with the formation of very elastic interfaces, could also have contributed to the formation and stability of these foams.

Pre-firing microstructures with very different features were developed using certain experimental conditions for each processing route. The developed microstructural characteristics were consistent with the rheological properties of the studied suspensions and the physicochemical and viscoelastic properties of these foamed suspensions.

Green disks shaped by the conventional route displayed high porosity, which did not markedly depend on the protein content. By this route, a cellular microstructure with typical features of a ceramic foam composed of a continuous solid three-dimensional network of struts with an acceptable degree of packing and mainly cells open with an almost spherical morphology separated by thin solid walls were developed. The cell size was strongly dependent on the protein content and could be decreased by increasing the protein content, which agrees with the parameters determined for bubble size distributions. In contrast, the window size turned out to be independent of the protein amount. In turn, in all the materials prepared by the methylcellulose route, the porosity ended up being lower than that achieved for materials prepared by the other route. A cellular microstructure with spherical, mainly closed cells and thicker walls than those formed in materials prepared by the other route was developed. In addition, struts with a good degree of packing appeared in a more isolated form. Window size was also independent of the cell size and turned out to be smaller than that obtained for the materials prepared by the conventionally reported route. The microstructural characteristics present in the majority of the materials indicated that the stability of the foams did not significantly vary during the thermal consolidation process.

A reduction in the ceramic loading used in the suspension with 10 vol% of protein and 0.5 wt% of methylcellulose allowed the development of green materials with much higher porosity

than that present in the material obtained by the conventionally reported route while preserving the cellular microstructure with typical features of ceramic foam as developed in the materials prepared by using only ceramic-protein suspensions.

## Acknowledgments

The authors gratefully acknowledge Dr. R. Moreno, Dr. M.I. Nieto and Ms. S. Benito (Instituto de Cerámica y Vidrio, CSIC, Madrid, España) for performing the measurements of pycnometric densities of the protein and polysaccharide powders used in this work. This study was funded by CONICET (Argentina) under project PIP 0936.

## References

- Dhara S, Bhargava P. A simple direct casting route to ceramic foams. *J Am Ceram Soc* 2003;**89**(10):1645–50.
- Luyten J, Mullens S, Coymans J, de Wilde AM, Thijs I, Kemps R. Different methods to synthesize ceramic foams. *J Eur Ceram Soc* 2009;**29**:829–32.
- Scheffler M, Colombo P, editors. *Cellular Ceramics: Structure, Manufacturing, Properties and Applications*. Weinheim: Wiley-VCH; 2005.
- Stuart AR, Gonzenbach UT, Tervoort E, Gauckler LJ. Processing routes to macroporous ceramics: a review. *J Am Ceram Soc* 2006;**89**:1771–89.
- Schneider H, Schreuer J, Hildmann B. Structure and properties of mullite—a review. *J Eur Ceram Soc* 2008;**28**(2):329–44.
- Osendi MI, Baudín C. Mechanical properties of mullite materials. *J Eur Ceram Soc* 1996;**16**(2):217–24.
- Orgaz F. Densification and crystallization kinetics of mullite diphasic gels from non-isothermal dilatometric experiments. *Bol Soc Esp Ceram* 2008;**47**:358–65.
- Montanaro L, Jorand Y, Fantozzi G, Negro A. Ceramics foams by powder processing. *J Eur Ceram Soc* 1998;**18**:1339–50.
- Kim H, Lee S, Han Y, Park J. Control of pore size in ceramic foams: Influence of surfactant concentration. *Mater Chem Phys* 2009;**113**:441–4.
- Gonzenbach UT, Stuart AR, Steinlin D, Tervoort E, Gauckler LJ. Macroporous ceramics from particle-stabilized wet foams. *J Am Ceram Soc* 2007;**90**:16–22.
- Lyckfeldt O, Brandt J, Lesca S. Protein forming—a novel shaping technique for ceramics. *J Eur Ceram Soc* 2000;**20**:2551–9.
- Garrn I, Reetz C, Brandes N, Kroh LW, Schubert H. Clot-forming: the use of proteins as binders for producing ceramic foams. *J Eur Ceram Soc* 2004;**24**:579–87.
- Bhattacharjee S, Besra L, Singh BP. Effect of additives on the microstructure of porous alumina. *J Eur Ceram Soc* 2007;**27**:47–52.
- Sandoval ML, Camerucci MA. Foaming performance of aqueous albumin and mullite-albumin systems used in cellular ceramic processing. *Ceram Int* 2014;**40**:1675–86.
- Talou MH, Camerucci MA. Two alternative routes for starch consolidation of mullite green bodies. *J Eur Ceram Soc* 2010;**30**(14):2881–7.
- Wojciechowska R, Wojciechowski W, Kaminski J. Thermal decompositions of ammonium and potassium alums. *J Therm Anal Calorim* 1988;**33**(2):503–9.
- Murayama K, Tomida M. Heat induced secondary structure and conformation change of bovine serum albumin investigated by Fourier transform infrared spectroscopy. *Biochemistry* 2004;**43**:11526–32.
- Damodaran S, Paraf A, editors. *Food proteins and their applications*. New York: Marcel Dekker; 1997.
- Rezwan K, Meier LP, Rezwan M, Vörös J, Textor M, Gauckler LJ. Bovine serum albumin adsorption onto colloidal Al<sub>2</sub>O<sub>3</sub>. Particles: a new model based on zeta potential and UV–vis measurements. *Langmuir* 2004;**20**:10055–61.
- Sandoval ML. *Desarrollo y caracterización de materiales celulares de mullite obtenidos por espumado y consolidación térmica con albúmina (Development and characterization of mullite foams obtained by foaming and thermal consolidation with albumin)*. National University of Mar del Plata; 2014 (Ph.D. Thesis).
- Tomšič M, Prossnigg F, Glatter O. A thermoreversible double gel: characterization of a methylcellulose and k-carrageenan mixed system in water by SAXS, DSC and rheology. *J Colloid Interface Sci* 2008;**322**:41–50.
- Kobayashi K, Huang C, Lodge TP. Thermoreversible gelation of aqueous methylcellulose solutions. *Macromolecules* 1999;**32**:7070–7.
- Raymundo A, Empis J, Sousa I. Method to evaluate foaming performance. *J Food Eng* 1998;**36**:445–52.
- Luck PJ, Bray N, Foegeding EA. Factors determining yield stress and overrun of whey protein foams. *J Food Sci* 2001;**67**:1677–81.
- Liang Y, Kristinsson HG. Influence of pH-induced unfolding and refolding of egg albumen on its foaming properties. *J Food Sci* 2005;**70**:C222–30.
- Schramm LL. *Emulsions, foams and suspensions: fundamentals and applications*. Weinheim: WILEY-VCH; 2005.
- Kato A, Takahashi A, Matsudomi N, Kobayashi K. Determination of foaming properties of proteins by conductivity measurements. *J Food Sci* 1983;**48**:62–5.
- Barigou M, Deshpande NS, Wiggers FN. An enhanced electrical resistance technique for foam drainage measurement. *Colloids Surf A Physicochem Eng Asp* 2001;**189**:237–46.
- Phianmongkhon A, Varley J. A multi point conductivity measurement system for characterization of protein foams. *Colloids Surf B Biointerfaces* 1999;**12**:247–59.
- Wright DJ, Hemmatt JW. Foaming properties of protein solutions: comparison of large-scale whipping and conductimetric methods. *J Sci Food Agric* 1987;**41**:361–71.
- Glaser LA, Paulson AT, Speers RA, Yada RY, Rousseau D. Foaming behavior of mixed bovine serum albumin-protamine systems. *Food Hydrocoll* 2007;**21**:495–506.
- Exerowa D, Kruglyakov PM. *Foam and foam films: theory, experiment, application*. Studies in interface science, 5. Amsterdam: Elsevier Science; 1998.
- Patino JM, Pilosof AM. Protein-polysaccharide interactions at fluid interfaces. *Food Hydrocoll* 2011;**25**:1925–37.
- Dhara S, Bhargava P. Influence of slurry characteristics on porosity and mechanical properties of alumina foams. *Int J Appl Ceram Technol* 2006;**3**(5):382–92.